Critical Role of the A^2 Amino Acid Residue in the Biological Activity of Insulin: [2-Glycine-A]- and [2-Alanine-A]insulins†

Kouki Kitagawa, Hiroshi Ogawa, G. Thompson Burke, Jacob D. Chanley, and Panayotis G. Katsoyannis*

ABSTRACT: We report the synthesis of [2-glycine-A]insulin ([Gly^2-A]insulin) and [2-alanine-A]insulin ([Ala^2-A]insulin) in which the indicated amino acid has been substituted for isoleucine found in this position in the natural hormone. The circular dichroic (CD) spectra of the analogues were obtained, and their properties were examined in several biological assays. CD studies suggested that the analogues remain monomeric at concentrations at which insulin is partly or mostly dimeric. Both analogues are extremely weak full agonists. [Gly^2-A]-insulin displays 0.05% of the potency of bovine insulin, whereas [Ala^2-A]insulin assays at 0.4% of the activity of the natural hormone. We conclude that the presence of the side chain of isoleucine at position A^2 is a critical requirement for high biological activity in insulin. The data, together with previous observations, are discussed in connection with an interaction between the side chain of isoleucine-A^2 and the phenolic ring system of tyrosine-A^{19}, which are in van der Waals contact in crystalline insulin. This interaction may be required to permit the molecule to assume a conformation consistent with dimerization and with binding to the insulin receptor.

The X-ray model of insulin indicates that the molecule is folded upon itself in such a way as to bring the C-terminal end of the A chain into proximity with the N-terminal end of this chain, placing the side chain of isoleucine-A^2 into van der Waals contact with the tyrosine residue at position A^{19} (Blundell et al., 1972). We have recently described an insulin analogue in which norleucine is substituted for isoleucine at position A^2 (Okada et al., 1981). This compound displays greatly reduced potency in biological assays, and we proposed that the substitution might have disrupted a vital interaction between residues A^2 and A^{19}. We could not, however, rule out the possibility that norleucine might disrupt the α-helical region formed by residues A^2–A^8. In this paper, we describe the synthesis and evaluation of two analogues in which the isoeleucine residue at position A^2 has been replaced by glycine or by alanine. The results indicate that the side chain of isoleucine plays a critical role in maintaining a structure commensurate with high biological activity. The interaction between isoleucine-A^2 and tyrosine-A^{19} will be discussed in a subsequent paper.

Experimental Procedures

Details of the synthetic and analytical procedures used are given in a previous paper (Schwartz et al., 1981). The homogeneity of the intermediate peptide derivatives was ascertained by TLC[1] on 6060 silica gel (Eastman chromagram sheet). The solvent systems used were 89:10:1 and 45:10:1 chloroform–methanol–water. Amino acid analyses were performed in a Beckman 119-CL analyzer equipped with a Model 126 data system. Acid hydrolyses were performed with 6 N HCl under nitrogen in the presence of phenol at 110 °C for 24 h. The preparation of the Cellex-E (BioRad Laboratories) column and the washing of the resin were carried out in exactly the same way as described previously in the preparation of the comparable ECTEOLA–cellulose column (Ferderigos et al., 1979). Isoelectric focusing on thin-layer plates was carried out as described previously (Schwartz et al., 1981). Paper prints of the electrograms were stained with Coomassie Brilliant Blue R250, but the stains faded quickly, and we were unable to obtain photographic copies. ^{125}I-insulin, 80–100 μCi/μg, and [3-^{3}H]glucose, 18 Ci/mmol, were purchased from New England Nuclear. Crystalline bovine insulin and fatty acid free bovine serum albumin were products of Sigma, and fraction V bovine serum albumin was from Schwarz/Mann. Crude collagenase, type II, was obtained from Worthington. The scintillation fluids Filtron-X and Soluscint-O were products of National Diagnostics. Type EGWP cellulose–acetate filters were purchased from Millipore, and antibodies for radioimmunoassay were products of Calbiochem-Behring.

Receptor Binding: Rat Liver Plasma Membranes. Triplicate 0.2-mL incubations contained ^{125}I-insulin, 3×10^{-10} M, unlabeled insulin or analogue as indicated, and plasma membranes (20–40 μg of protein) prepared essentially as described earlier (Horvat et al., 1975), in 0.1 M sodium phosphate, pH 7.4, containing 0.6% fraction V bovine serum albumin. Following incubation for 45 min at 24 °C, the mixtures were diluted with 2.0 mL of 0.1 M sodium phosphate, pH 7.4, containing 0.1% fraction V bovine serum albumin, ice cold, and immediately filtered through cellulose–acetate filters. The filters were washed with the two portions of the ice-cold buffer, dried, and counted in Filtron-X. Nonspecific binding, defined as radioactivity remaining on the filters when the incubations contained 1×10^{-5} M unlabeled insulin, was subtracted from all values. Relative potency was obtained as the concentration ratio of unlabeled insulin to analogue required to inhibit 50% of the specific binding of ^{125}I-insulin to the receptor preparation.

Lipogenesis: Conversion of [3-^{3}H]Glucose into Lipids. Adipocytes were prepared by incubating epididymal and perirenal flat pads obtained from male rats weighing 200–300 g with 1.0 mg/mL collagenase for 60 min at 37 °C, followed by filtration through gauze and then through fine-mesh silk. Cells were washed twice by flotation in a clinical centrifuge

† From the Department of Biochemistry, Mount Sinai School of Medicine, City University of New York, New York, New York 10029. *Received August 4, 1983.* This work was supported by the National Institute of Arthritis, Diabetes, Digestive and Kidney Diseases, U.S. Public Health Service (AM12925). For the previous paper of this series, see Schwartz et al. (1983).

[1] Abbreviations: CM, carboxymethyl; DMF, dimethylformamide; Me_2SO, dimethyl sulfoxide; TEA, triethylamine; Tris-HCl, 2-amino-2-(hydroxymethyl)-1,3-propanediol hydrochloride; TLC, thin-layer chromatography.

0006-2960/84/0423-1405$01.50/0

before suspension for use. The incubation medium was Krebs–Ringer bicarbonate containing half the recommended calcium, 0.5 mM glucose, and 3% fatty acid free bovine serum albumin, with 95% O_2–5% CO_2 as the gas phase. Triplicate lipogenesis incubations contained 1.0 mL of adipocyte suspension (20–40 mg dry wt cells) and insulin or analogue as indicated. Cells were preincubated for 45 min at 37 °C before the addition of [3-^{3}H]glucose. Incubation was continued for 60 min and stopped by the addition of 0.2 mL of 5 N H_2SO_4 and 0.2 mL of corn oil to aid in the extraction of lipids. Samples were extracted with 10 mL of Soluscint-O for 30 min at room temperature before being counted. Under these conditions, [3-^{3}H]glucose is not extracted into the organic phase containing the fluors and is essentially uncounted. Zero and 100% stimulation of lipogenesis are defined as radioactivity observed in the absence and presence, respectively, of 9.1×10^{-10} M insulin (5.5 ng/mL). Relative potency was obtained as the concentration ratio of insulin to analogue required to produce 50% of the maximum stimulation of lipogenesis.

Radioimmunoassay. Guinea pig antiserum to porcine insulin and goat anti-guinea pig γ-globulin were used at 1:25 dilution in assay buffer (sodium phosphate, 0.04 M, pH 7.6, containing 0.154 M NaCl, 0.1% gelatin, and 0.01% thimerosal). Duplicate assay tubes contained 0.1 mL of anti-insulin antiserum, 0.072 ng of ^{125}I-insulin, and bovine insulin (0.06–0.36 ng) or synthetic analogue (1–4.0 ng) as indicated in individual experiments, in a total volume of 0.8 mL. After incubation at room temperature overnight, the precipitating antibody, 0.2 mL, was added, and the tubes were further incubated overnight at room temperature. Immune precipitates were collected on cellulose–acetate filters and washed with two successive 1.0-mL portions of ice-cold assay buffer. Filters were dried and counted in Filtron-X. Straight-line plots of C_0/C_i (Hales & Randle, 1963) were constructed by linear regression analysis, and the potency of an analogue relative to bovine insulin was obtained as the ratio of the slopes of such plots.

Circular Dichroism (CD). The CD measurements of the analogues and zinc-free insulin were obtained with a JASCO J-500A recording spectrophotometer equipped with a data processor. Spectra were taken at 25 °C under nitrogen in 0.001 M HCl with protein concentrations of ca. 0.005–1.0 mg/mL. Cylindrical quartz cells with optical path lengths of 0.10–10.00 cm were used. Each sample was scanned 4 or 8 times, and an average spectrum was obtained by using the data processor and correcting for the base line. Mean residue ellipticity ($[\theta]^{mrw}$) was calculated from

$$[\theta]^{mrw} = \theta\bar{M}/(cl)$$

where θ is the observed ellipticity, $\bar{M}$ is the mean residue molecular weight (mrw) calculated to be 112 for insulin and analogues, c is the protein concentration in milligrams per milliliter, and l is the optical path length in centimeters.

General Aspects of Synthesis of Sheep [Gly^2-A]- and [Ala^2-A]insulins. These analogues were synthesized by the interaction of the S-sulfonated bovine (sheep) B chain with the thiol form of [Gly^2]A and [Ala^2]A chains of sheep insulin, respectively. The latter compounds were obtained by reduction with 2-mercaptoethanol of the S-sulfonated derivatives of the respective chains. The synthesis of the S-sulfonated [Gly^2]A (X) and [Ala^2]A (XI) chains, patterned after our synthesis of the sheep A chain (Katsoyannis et al., 1966b), involved as the key intermediates the construction of the protected heneicosapeptides VIII and IX containing the entire amino acid sequence of the sheep [Gly^2]A and [Ala^2]A chains, respectively. The synthesis involved the coupling of the C-terminal tridecapeptide (sequence A^9–A^{21}) with the adjacent tetrapeptide (sequence A^5–A^8) to produce the C-terminal heptadecapeptide (VII) (sequence A^5–A^{21}), which in turn were coupled with the N-terminal tetrapeptides (III or VI) (sequence A^1–A^4) to yield the protected heneicosapeptides VIII and IX, respectively. Removal of the blocking groups, and sulfitolysis of the resulting thiol derivatives produced the S-sulfonated [Gly^2]A and [Ala^2]A chains.

N-(Benzyloxycarbonyl)glycyl-L-valyl-γ-tert-butyl-L-glutamic Acid Methyl Ester (I). N-(Benzyloxycarbonyl)-L-valyl-γ-*tert*-butyl-L-glutamic acid methyl ester (Katsoyannis et al., 1966a) (13.8 g) was dissolved in methanol (100 mL) and hydrogenated for 5 h in the presence of 10% palladium–charcoal catalyst (3 g). The catalyst was filtered off and the filtrate concentrated to dryness in vacuo. The residue was dissolved in DMF (20 mL), and to this solution was added N-(benzyloxycarbonyl)glycine *p*-nitrophenyl ester (Iselin et al., 1957) (9.9 g) dissolved in tetrahydrofuran (50 mL) followed by the addition of a few drops of TEA to ensure basicity. After 24 h, the mixture was concentrated to a small volume under reduced pressure and then diluted with ethyl acetate (400 mL) and water (100 mL). The organic layer was washed successively with 10% citric acid, 5% Na_2CO_3, and water, dried, and concentrated to a small volume. Addition of petroleum ether caused the precipitation of the product. For purification, this product was dissolved in chloroform (10 mL) and placed on a silica gel 60 column (7.0 × 12.0 cm) that was equilibrated with chloroform. The column was first eluted with chloroform and then with chloroform–methanol (95:5 v/v). The effluent containing the described product [as detected by TLC, R_f 0.45, using the solvent system chloroform–methanol–acetic acid (9:1:0.5 v/v)] was concentrated to a small volume and mixed with petroleum ether. The precipitated product was collected by filtration: wt 7.15 g (47%); mp 112–116 °C; $[\alpha]^{25}_D$ −35.6° (*c* 1, methanol). It was homogeneous on TLC. Anal. Calcd for $C_{25}H_{37}N_3O_8$: C, 59.1; H, 7.35; N, 8.3. Found: C, 59.1; H, 7.61; N, 8.4.

N-(Benzyloxycarbonyl)glycylglycyl-L-valyl-γ-tert-butyl-L-glutamic Acid Methyl Ester (II). A solution of compound I (5.07 g) in methanol (80 mL) was hydrogenated for 3 h over 10% palladium–charcoal catalyst (1.5 g). The catalyst was filtered off and the filtrate concentrated to dryness. To a solution of the residue in DMF (20 mL) was added N-(benzyloxycarbonyl)glycine *p*-nitrophenyl ester followed by a few drops of TEA. After 24 h, the mixture was poured into ethyl acetate (300 mL) and water (100 mL). The organic layer was washed (10% citric acid, 5% Na_2CO_3, and water) and dried. After evaporation of the solvent, the remaining product was crystallized upon trituration with ether and recrystallized from methanol–ether: wt 5.2 g (92%); mp 100–150 °C; $[\alpha]^{25}_D$ −28.4° (*c* 1, methanol). It was homogeneous on TLC. Anal. Calcd for $C_{27}H_{40}N_4O_9$: C, 57.4; H, 7.14; N, 9.9. Found: C, 57.2; H, 7.23; N, 9.6.

N-(Benzyloxycarbonyl)glycylglycyl-L-valyl-γ-tert-butyl-L-glutamic Acid Hydrazide (III). A solution of compound II (3.95 g) in warm methanol (40 mL) was cooled to room temperature and mixed with hydrazide hydrate (4 mL). After 48 h, the precipitated product was filtered off, washed with cold methanol and water, and dried: wt 3.5 g (88%); mp 181–183 °C; $[\alpha]^{25}_D$ −11.2° (*c* 1, DMF). It was homogeneous on TLC. Anal. Calcd for $C_{26}H_{40}N_6O_8$: C, 55.3; H, 7.14; N, 14.9. Found: C, 55.0; H, 7.09; N, 14.6.

N-(Benzyloxycarbonyl)-L-alanyl-L-valyl-γ-tert-butyl-L-glutamic Acid Methyl Ester (IV). N-(Benzyloxycarbonyl)-L-valyl-γ-*tert*-butyl-L-glutamic acid methyl ester (9.0

g) was dissolved in methanol (100 mL) and hydrogenated for 5 h over 10% palladium–charcoal catalyst (1.5 g). After removal of the catalyst and evaporation of the solvent to dryness, the residue was dissolved in DMF (20 mL). To this solution was added *N*-(benzyloxycarbonyl)-L-alanine *p*-nitrophenyl ester (Goodman & Steuben, 1959) (6.9 g) followed by a few drops of TEA. The reaction mixture was stirred for 25 h, concentrated to a small volume under reduced pressure, and then diluted with ethyl acetate (400 mL) and water (100 mL). The organic layer was washed (5% Na_2CO_3, 10% citric acid, and water), dried, and concentrated to a small volume. Addition of petroleum ether caused the precipitation of the product, which was isolated and purified by silica gel chromatography as described in the synthesis of compound I: wt 5.4 g (52%); mp 143–145 °C; $[\alpha]^{25}_D$ −54.9° (*c* 1, methanol). It was homogeneous on TLC. Anal. Calcd for $C_{26}H_{39}N_3O_8$: C, 59.9; H, 7.54; N, 8.1. Found: C, 60.0; H, 7.65; N, 7.9.

N-(Benzyloxycarbonyl)glycyl-L-alanyl-L-valyl-γ-tert-butyl-L-glutamic Acid Methyl Ester (*V*). A solution of compound IV (5.2 g) in methanol (80 mL) was hydrogenated for 3 h over 10% palladium–charcoal catalyst (1.5 g). After removal of the catalyst and evaporation of the solvent, the residue was dissolved in DMF (20 mL), and to this solution was added *N*-(benzyloxycarbonyl)glycine *p*-nitrophenyl ester (3.3 g) followed by a few drops of TEA. The reaction mixture was then processed as described in the synthesis of compound II: wt 4.3 g (74%); mp 141–145 °C; $[\alpha]^{25}_D$ −56.0° (*c* 1, methanol). It was homogeneous on TLC. Anal. Calcd for $C_{28}H_{42}N_4O_9$: C, 58.1; H, 7.32; N, 9.7. Found: C, 58.2; H, 7.59; N, 9.8.

N-(Benzyloxycarbonyl)glycyl-L-alanyl-L-valyl-γ-tert-butyl-L-glutamic Acid Hydrazide (*VI*). This derivative was prepared from compound V (3.47 g), methanol (30 mL), and hydrazine hydrate (2.5 mL) by the exact procedure used in the synthesis of compound III: wt 2.85 g (82%); mp 215–219 °C; $[\alpha]^{25}_D$ −19.44° (*c* 1, DMF). It was homogeneous on TLC. Anal. Calcd for $C_{27}H_{42}N_6O_8$: C, 56.0; H, 7.32; N, 14.5. Found: C, 55.9; H, 7.33; N, 14.3.

N-(tert-Butoxycarbonyl)-L-glutaminyl-S-benzyl-L-cysteinyl-S-benzyl-L-cysteinyl-L-alanylglycyl-L-valyl-S-benzyl-L-cysteinyl-L-seryl-L-leucyl-L-tyrosyl-L-glutaminyl-L-leucyl-γ-benzyl-L-glutamyl-L-asparaginyl-O-benzyl-L-tyrosyl-S-benzyl-L-cysteinyl-L-asparagine p-Nitrobenzyl Ester (*VII*). A solution of *N*-(*tert*-butoxycarbonyl)glycyl-L-valyl-*S*-benzyl-L-cysteinyl-L-seryl-L-leucyl-L-tyrosyl-L-glutaminyl-L-leucyl-γ-benzyl-L-glutamyl-L-asparaginyl-*O*-benzyl-L-tyrosyl-*S*-benzyl-L-cysteinyl-L-asparagine *p*-nitrobenzyl ester (Ferderigos et al., 1983) (2.1 g) in a mixture of trifluoroacetic acid and acetic acid (7:3 v/v; 20 mL) was stored at room temperature for 45 min and then poured into ether (300 mL). The precipitated partially deblocked tridecapeptide was filtered off, washed with ether, and dried over KOH in vacuo. To a cold (0 °C) solution of this product in a mixture of DMF (20 mL) and Me_2SO (30 mL) containing TEA (0.14 mL) was added the tetrapeptide azide prepared as follows. The protected tetrapeptide hydrazide *N*-(*tert*-butoxycarbonyl)-L-glutaminyl-*S*-benzyl-L-cysteinyl-*S*-benzyl-L-cysteinyl-L-alanine hydrazide (Okada & Katsoyannis, 1975) (2.16 g) was dissolved in DMF (30 mL), and to this solution, cooled to −10 °C, was added 4.67 N HCl in DMF (1.3 mL) followed by isoamyl nitrite (0.4 mL). After 10 min at −10 °C, the mixture was cooled to −30 °C, neutralized with TEA (0.84 mL), and added to the solution of the deblocked tridecapeptide prepared as described previously. After 48 h at 4 °C, the reaction mixture was condensed under reduced pressure to half of its original volume and then poured into methanol (300 mL). The precipitated protected heptadecapeptide was filtered off, washed with methanol, and reprecipitated from a solution in Me_2SO by the addition of water: wt 2.15 g (80%); mp 275–280 °C dec; $[\alpha]^{25}_D$ −37.9° (*c* 1, hexamethylphosphoramide). Anal. Calcd for $C_{132}H_{168}N_{22}O_{31}S_4$: C, 59.0; H, 6.30; N, 11.5. Found: C, 59.0; H, 6.55; N, 11.4. Amino acid analysis after acid hydrolysis gave the following composition expressed in molar ratios: $Asp_{2.1(2)}Ser_{0.9(1)}Glu_{3.2(3)}Gly_{1.0(1)}Ala_{1.0(1)}Val_{0.9(1)}Leu_{1.9(2)}Tyr_{1.8(2)}$*S*-Bzl-$Cys_{3.1(4)}$ (average amino acid recovery 90%).

N-(Benzyloxycarbonyl)glycylglycyl-L-valyl-γ-tert-butyl-L-glutamyl-L-glutaminyl-S-benzyl-L-cysteinyl-S-benzyl-L-cysteinyl-L-alanylglycyl-L-valyl-S-benzyl-L-cysteinyl-L-seryl-L-leucyl-L-tyrosyl-L-glutaminyl-L-leucyl-γ-benzyl-L-glutamyl-L-asparaginyl-O-benzyl-L-tyrosyl-S-benzyl-L-cysteinyl-L-asparagine p-Nitrobenzyl Ester (*VIII*). The protected heptadecapeptide VII (1.34 g) was deblocked with a mixture of trifluoroacetic acid–acetic acid (7:3; 10 mL) as described in the synthesis of compound VII. The resulting trifluoroacetate salt of the deblocked peptide was dissolved in a mixture of DMF (15 mL) and Me_2SO (15 mL) containing TEA (0.07 mL), and to this solution, cooled to 0 °C, was added the tetrapeptide azide, prepared from the hydrazide III (0.71 g) as described in the synthesis of compound VII. The following reagents were used for this reaction: DMF (10 mL), 4.67 N HCl in DMF (0.54 mL), isoamyl nitrite (0.17 mL), and TEA (0.35 mL). After 48 h at 4 °C, the reaction mixture was poured into methanol (500 mL), and the precipitated product was collected by centrifugation, washed with methanol, and dried: wt 1.29 g (86%); mp > 270 °C; $[\alpha]^{25}_D$ 27.8° (*c* 1, hexamethylphosphoramide). Amino acid analysis of an acid hydrolysate gave the following molar ratios: $Asp_{2.0(2)}Ser_{0.9(1)}Glu_{4.1(4)}Gly_{3.0(3)}Ala_{1.0(1)}Val_{1.8(2)}Leu_{1.9(2)}Tyr_{1.8(2)}$*S*-Bzl-$Cys_{3.7(4)}$ (average amino acid recovery 90%).

N-(Benzyloxycarbonyl)glycyl-L-alanyl-L-valyl-γ-tert-butyl-L-glutamyl-L-glutaminyl-S-benzyl-L-cysteinyl-S-benzyl-L-cysteinyl-L-alanylglycyl-L-valyl-S-benzyl-L-cysteinyl-L-seryl-L-leucyl-L-tyrosyl-L-glutaminyl-L-leucyl-γ-benzyl-L-glutamyl-L-asparaginyl-O-benzyl-L-tyrosyl-S-benzyl-L-cysteinyl-L-asparagine p-Nitrobenzyl Ester (*IX*). The protected heptadecapeptide VII (1.34 g) was deblocked as described in the synthesis of compound VIII. To a cold (0 °C) solution of the deblocked product in a mixture of DMF (15 mL) and Me_2SO (15 mL) containing TEA (0.07 mL) was added the tetrapeptide azide prepared from the corresponding hydrazide VI (0.73 g) as described in the synthesis of compound VII. The reagents used for this reaction were exactly the same as those used in the synthesis of compound VIII. The reaction mixture was processed as described in the synthesis of compound VIII: wt 1.3 g (87%); mp >270 °C; $[\alpha]^{25}_D$ −36.6° (*c* 1, hexamethylphosphoramide). Amino acid analysis of an acid hydrolysate gave the following molar ratios: $Asp_{1.9(2)}Ser_{0.8(1)}Glu_{4.2(4)}Gly_{2.0(2)}Ala_{1.9(2)}Val_{2.0(2)}Leu_{1.9(2)}Tyr_{1.8(2)}$*S*-Bzl$Cys_{3.6(4)}$ (average amino acid recovery 97%).

Glycylglycyl-L-valyl-L-glutamyl-L-glutaminyl-S-sulfo-L-cysteinyl-S-sulfo-L-cysteinyl-L-alanylglycyl-L-valyl-S-sulfo-L-cysteinyl-L-seryl-L-leucyl-L-tyrosyl-L-glutaminyl-L-leucyl-L-glutamyl-L-asparaginyl-L-tyrosyl-S-sulfo-L-cysteinyl-L-asparagine (*Sheep Insulin [Gly²]A Chain S-Sulfonate*) (*X*). A solution of the protected heneicosapeptide VIII (0.34 g) in trifluoroacetic acid (3 mL) and anisole (0.7 mL) was stored at 0 °C for 20 min and at room temperature for 40 min and then poured into ether (150 mL). The precipitated partially protected heneicosapeptide was collected by centrifugation,

Table I: Amino Acid Composition[a] of an Acid Hydrolysate and an Enzymatic Digest (Aminopeptidase M) of the S-Sulfonated [Gly²]A and [Ala²]A Chains

	[Gly²]A chain *S*-sulfonate				[Ala²]A chain *S*-sulfonate			
	acid hydrolysis		enzymatic hydrolysis		acid hydrolysis		enzymatic hydrolysis	
amino acid	theory	found	theory	found	theory	found	theory	found
Asp	2	2.0	0	0	2	2.0	0	0
Ser	1	0.9	1	*b*	1	0.9	1	*b*
Asn	0	0	2	*b*	0	0	2	*b*
Gln	0	0	2	*b*	0	0	2	*b*
Glu	4	4.0	2	2.2	4	4.0	2	1.7
Gly	3	3.0	3	2.9	2	2.0	2	1.8
Ala	1	1.0	1	1.1	2	2.0	2	2.0
Val	2	1.9	2	1.9	2	2.0	2	1.9
½-Cys	4	nd[c]	0	0	4	nd	0	0
Leu	2	2.0	2	2.0	2	2.0	2	2.0
Tyr	2	1.9	2	2.0	2	1.9	2	1.7
S-sulfo-Cys	0	0	4	3.9	0	0	4	3.8

[a] Number of amino acid residues per molecule. [b] Emerge on the same position and not determined. [c] nd, not determined.

washed with ether, and dried over KOH in vacuo: wt 284 mg. The total deprotection of this product with sodium in liquid ammonia (200 mL) was carried out as described previously (Katsoyannis et al., 1966b). After evaporation of the ammonia, the residue was dissolved in 8 M guanidine hydrochloride (25 mL), and to this solution, adjusted to pH 8.9 with acetic acid or dilute NH_4OH (depending on the pH of the solution), were added sodium sulfite (1.18 g) and freshly prepared sodium tetrathionate (0.56 g). The mixture was stirred at room temperature for 3.5 h and then dialyzed in Spectrapor membrane tubing No. 3 at 4 °C for 24 h against four changes of distilled water (4 L each). Lyophilization of the dialysate afforded the crude [Gly²]A chain *S*-sulfonate, which was then dissolved in 0.015 M NH_4HCO_3 (4 mL) and chromatographed on a Sephadex G-15 column (4.5 × 44 cm) equilibrated and eluted with 0.015 M NH_4HCO_3 at a flow rate of 60 mL/h. The effluent corresponding to the main peak (230–320 mL), as monitored by an ISCO spectrophotometer (Model UA-5), was lyophilized, and the [Gly²]A chain *S*-sulfonate was obtained as a white fluffy powder: wt 184 mg. For purification, this material (63 mg) was dissolved in 0.1 M Tris-HCl buffer (pH 7.0; 3 mL) and placed on a Cellex-E column (1.2 × 45 cm), which was equilibrated with the same buffer and eluted with application of a linear NaCl gradient (flow rate 75 mL/h) as described previously (Ferderigos et al., 1979). The elution pattern of this column was monitored by an ISCO spectrophotometer and a conductivity meter (Radiometer, Copenhagen). The eluate under the main peak (480–660 mL) was collected, dialyzed in Spectrapor membrane tubing No. 3 as described above, and lyophilized. The product obtained (52 mg) was dissolved in 0.1 M Tris-HCl buffer (pH 7.0; 3 mL) and rechromatographed on the same Cellex-E column and under identical conditions as described above. From the effluent (350–500 mL), after dialysis and lyophilization, [Gly²]A chain *S*-sulfonate was obtained in highly purified form: wt 48 mg.

On thin-layer electrophoresis (precoated silica gel 60, Merck Co.) in 2 N acetic acid–0.6 N formic acid (1:1 v/v), pH 2.0 and 480 V, the synthetic chain analogue moved as a single component (data not shown). Amino acid analysis of the purified product after acid hydrolysis gave a composition expressed in molar ratios, shown in Table I, in good agreement with the expected values. Digestion of the synthetic chain with aminopeptidase M and amino acid analysis of the digest gave the composition shown in Table I. It is apparent that the [Gly²]A chain *S*-sulfonate was completely digested by the enzyme, indicating that the stereochemical purity of the constituent amino acid was preserved during the synthetic processes.

Glycyl-L-*alanyl*-L-*valyl*-L-*glutamyl*-L-*glutaminyl*-*S*-*sulfo*-L-*cysteinyl*-*S*-*sulfo*-L-*cysteinyl*-L-*alanylglycyl*-L-*valyl*-*S*-*sulfo*-L-*cysteinyl*-L-*seryl*-L-*leucyl*-L-*tyrosyl*-L-*glutaminyl*-L-*leucyl*-L-*glutamyl*-L-*asparaginyl*-L-*tyrosyl*-*S*-*sulfo*-L-*cysteinyl*-L-*asparagine* (*Sheep Insulin* [*Ala*²]*A Chain S-Sulfonate*) (*XI*). Deblocking of the protected heneicosapeptide IX (0.3 g) with TFA and sodium in liquid ammonia and sulfitolysis of the reduced product were carried out in exactly the same way as described in the synthesis of compound X. After Sephadex G-15 chromatography and lyophilization, 189 mg of [Ala²]A chain *S*-sulfonate was obtained. For purification, this product (68 mg) was chromatographed on a Cellex-E column with 0.1 M Tris-HCl buffer (pH 7.0) and a linear NaCl gradient as described in the synthesis of compound X. The eluate under the main peak (395–515 mL of effluent) was dialyzed and lyophilized, and the material obtained was rechromatographed on the same Cellex-E column and under identical conditions as described above. From the effluent (410–530 mL) after dialysis and lyophilization, [Ala²]A chain *S*-sulfonate was obtained in highly purified form: wt 33 mg.

On thin-layer electrophoresis (precoated TLC plates, 10 × 20 cm, silica gel 60; EM Laboratories) in a 2 N acetic acid–0.6 N formic acid mixture (1:1 v/v), pH 2.0 and 480 V, the synthetic chain analogue moved as a single band (Pauly reaction; data not shown). Amino acid analysis after acid hydrolysis and aminopeptidase M digestion gave the molar ratios shown in Table I in good agreement with the theoretically expected values.

S-Sulfonated Derivative of the B Chain of Sheep Insulin. The B chain of sheep insulin is identical with the corresponding chain of bovine insulin (Sanger & Tuppy, 1951; Brown et al., 1955). The bovine (sheep) B chain *S*-sulfonate was prepared by oxidative sulfitolysis of bovine insulin followed by separation of the resulting A and B chain *S*-sulfonates by CM-cellulose chromatography as we have reported previously (Katsoyannis et al., 1967a).

Synthesis and Isolation of [*Gly*²]*A Sheep Insulin.* This insulin analogue was synthesized by the interaction of the sulfhydryl form of [Gly²]A chain with the S-sulfonated form of the bovine (sheep) B chain by the procedures we have described previously (Katsoyannis & Tometsko, 1966; Katsoyannis et al., 1967b,c; Schwartz & Katsoyannis, 1976). Briefly, 20 mg of [Gly²]A chain *S*-sulfonate was converted to the sulfhydryl form on exposure to 2-mercaptoethanol (in 5 mL of 0.1 M Tris-HCl buffer, pH 8.3 at 37 °C, 8 min) and

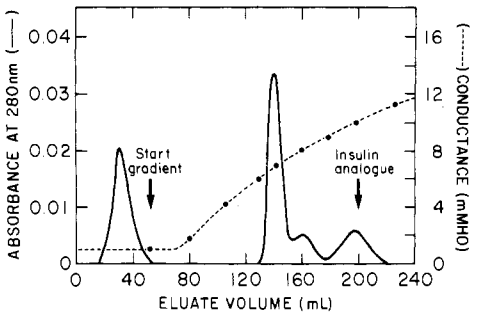

FIGURE 1: Chromatography of a combination mixture (see Experimental Procedures) of the sulfhydryl form of sheep [Gly^2]A chain with the S-sulfonated sheep (bovine) B chain on a 0.9 × 23 cm CM-cellulose column with acetate buffer (Na^+, 0.024 M, pH 3.3) and an exponential NaCl gradient. The column effluent was monitored with an ISCO recording spectrophotometer and a conductivity meter. The [Gly^2-A]insulin (175–220 mL of effluent) was recovered as the hydrochloride.

Table II: Amino Acid Composition[a] of an Acid Hydrolysate of Sheep [Gly^2-A]- and [Ala^2-A]insulin

	[Gly^2-A]insulin		[Ala^2-A]insulin	
amino acid	theory	found	theory	found
Lys	1	1.0	1	1.0
His	2	1.8	2	1.8
Arg	1	0.9	1	0.9
Asp	3	3.0	3	3.1
Thr	1	0.9	1	1.0
Ser	2	2.0	2	2.2
Pro	1	0.9	1	0.9
Glu	7	6.9	7	7.1
Gly	6	5.8	5	5.0
Ala	3	3.0	4	3.9
$^1/_2$-Cys	6	nd[b]	6	nd[b]
Val	5	4.7	5	4.9
Leu	6	6.0	6	6.2
Tyr	4	3.9	4	3.9
Phe	3	3.0	3	3.0

[a] Number of amino acid residues per molecule. [b] nd, not determined.

then allowed to react with 5 mg of B chain *S*-sulfonate for 20 h at pH 10.6 and 4 °C. The combination mixture was then processed as described previously (Katsoyannis et al., 1967b,c). Isolation of the insulin analogue from the reaction mixture was accomplished by chromatography on a 0.9 × 23 cm CM-cellulose column with an acetate buffer (Na^+ 0.024 M; pH 3.3) and exponential NaCl gradient as reported previously (Katsoyannis et al., 1967c). The chromatographic profile, as monitored by an ISCO spectrophotometer and by a conductivity meter (Radiometer, Copenhagen), is shown in Figure 1. The effluent containing the insulin analogue (175–220 mL) was processed as described previously (Katsoyannis et al., 1967c), and the [Gly^2-A]insulin was isolated via picrate as the hydrochloride (0.8 mg).

Amino acid analysis of this analogue after acid hydrolysis gave a composition expressed in molar ratios, shown in Table II, in good agreement with theoretically expected values. On isoelectric focusing on thin-layer plates in a 1:1 mixture of pH 3–10 and pH 4–6 ampholytes, [Gly^2-A] insulin focused into one band (data not shown).

Synthesis and Isolation of Sheep [Ala^2-A]insulin. The synthesis of this analogue by the interaction of the thiol form of [Ala^2]A chain and the S-sulfonated form of the bovine (sheep) B chain and its isolation were accomplished by exactly the same procedure outlined above in the synthesis of [Gly^2-A]insulin. Chromatography of a combination mixture of 20 mg of [Ala^2]A chain *S*-sulfonate and 5 mg of bovine

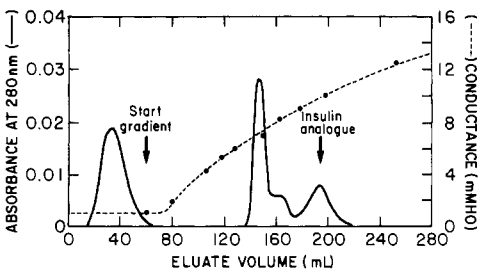

FIGURE 2: Chromatography of a combination mixture (see Experimental Procedures) of the sulfhydryl form of sheep [Ala^2]A chain with the S-sulfonated sheep (bovine) B chain on a 0.9 × 23 cm CM-cellulose column with acetate buffer (Na^+, 0.024 M, pH 3.3) and an exponential NaCl gradient. The column effluent was monitored with an ISCO recording spectrophotometer and a conductivity meter. The [Ala^2-A]insulin (175–220 mL of effluent) was recovered as the hydrochloride.

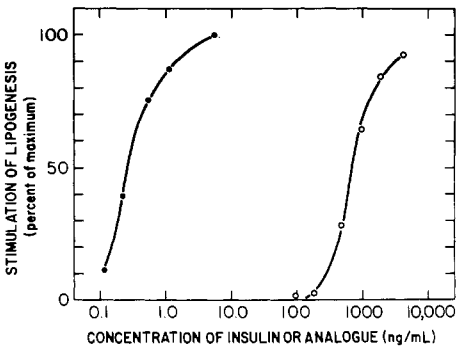

FIGURE 3: Effect of bovine insulin (●) and [Gly^2-A]insulin (○) on lipogenesis in rat adipocytes (see Experimental Procedures). The stimulation of lipogenesis, expressed as percent of maximum, is plotted as a function of the concentration of insulin and analogue. The data are from a representative experiment that was performed 3 times.

(sheep) B chain *S*-sulfonate gave the pattern shown in Figure 2. The [Ala^2-A]insulin was isolated from the effluent (175–220 mL) via picrate as the hydrochloride (0.6 mg).

Amino acid analysis of an acid hydrolysate of this analogue gave the ratios shown in Table II, in good agreement with theoretically expected values. On isoelectric focusing on thin-layer plates in a 1:1 mixture of pH 3–10 and pH 4–6 ampholytes, [Ala^2-A]insulin focused into one band (data not shown).

Biological Evaluation of [Gly^2-A]- and [Ala^2-A]insulins. The ability of [Gly^{2}A]insulin to stimulate lipogenesis is depicted in Figure 3. The analogue is a full agonist, reaching the same maximum stimulation of conversion of labeled glucose into organic-extractable material as is observed with bovine insulin. The concentration of analogue required to effect 50% of the maximum conversion, however, is vastly greater than the concentration of insulin that gives 50% maximum stimulation. The calculated relative potency of [Gly^{2}A]insulin is 0.05%, which makes this compound the weakest full agonist we have observed.

The behavior of [Ala^{2}A]insulin in lipogenesis is shown in Figure 4. Full agonist behavior is again evident, and the calculated relative potency is 0.4%, substantially higher than [Gly^{2}A]insulin, but still very low.

No dose–response curve is presented for receptor binding assays of [Gly^2-A]insulin; less than 50% of maximum inhibition of ^{125}I-insulin binding was achieved at the highest concentration attainable with the materials available (25 μg/mL).

Figure 5 shows the behavior of [Ala^2-A]insulin in receptor binding assays. Fifty percent of the maximum inhibition of ^{125}I-insulin is achieved for this compound, and its relative potency is calculated at 0.17%. While this figure is lower than

Table III: Mean Residue Weight Ellipticity of Insulin and Analogues at Selected Wavelengths as a Function of Concentration and Ratio of Ellipticities at 208 and 222 nm and 195 and 208 nm

compd	concn (μM)	10^{-3} deg cm^2 dmol^{-1}				$[\theta]_{208}/[\theta]_{222}$	$[\theta]_{195}/[\theta]_{208}$
		$[\theta]_{194.5}$	$[\theta]_{208}$	$[\theta]_{222}$	$[\theta]_{274}$		
insulin	168.5				230		
	16.85	22.2	13.5	10.3	195	1.31	1.64
	11.40	21.0	11.8	9.6		1.23	1.78
	8.42	19.3	12.3	8.9		1.36	1.56
	1.68	16.9	12.0	7.8	154	1.54	1.41
	1.14	13.8	11.2	7.2		1.56	1.23
	0.842	14.5	11.5	6.9		1.66	1.23
	0.168	(10.0)	(9.2)	(5.9)		(1.56)	(1.08)
[Gly^2-A]insulin[a]	12.0	11.4	11.2	6.9	163	1.62	1.02
[Ala^2-A]insulin[a]	14.0	11.4	11.0	6.9	145	1.58	1.04
[Nle^2-A]insulin[a,b]	17.4	11.2	11.2	6.7	100	1.67	1.00

[a] For this compound, $[\theta]$ refers to 193, 207, 220, and 268–269 nm. [b] See Okada et al. (1981).

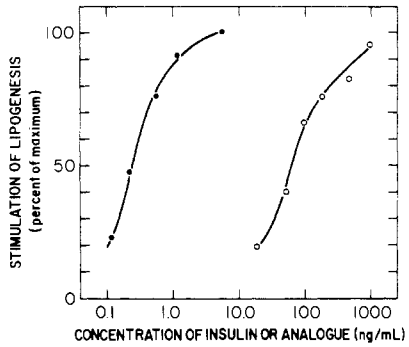

FIGURE 4: Effect of bovine insulin (●) and [Ala^2-A]insulin (○) on lipogenesis in rat adipocytes (see Experimental Procedures). The stimulation of lipogenesis, expressed as percent of maximum, is plotted as a function of the concentration of insulin and analogue. The data are from a representative experiment that was performed 3 times.

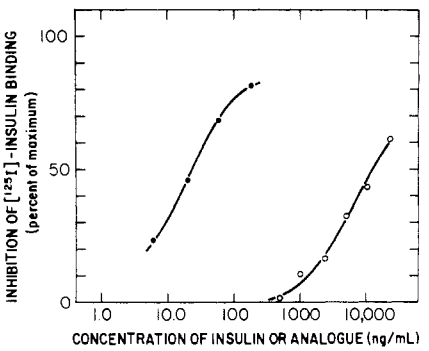

FIGURE 5: Effect of bovine insulin (●) and [Ala^2-A]insulin (○) on porcine ^{125}I-insulin binding to rat liver plasma membranes (see Experimental Procedures). The inhibition of ^{125}I-insulin binding, expressed as percent of maximum, is plotted as a function of the concentration of unlabeled bovine insulin and analogue. The data were obtained in a single experiment.

the potency obtained in lipogenesis assays, we do not consider the difference significant. The assay was run only once, in order to conserve analogue for other analyses, and it is difficult to ascribe physiological meaning to the difference at this very low potency. Both [Gly^2-A]insulin and [Ala^2-A]insulin were compared with bovine insulin in radioimmunoassay. Both analogues produced good straight-line plots of C_0/C_i (Hales & Randle, 1963) (data not shown), and their relative potencies are almost identical at 12.6–12.7% relative to bovine insulin.

Circular Dichroic Studies. Figure 6 illustrates the near- and far-ultraviolet CD spectra of the [Gly^2]A and [Ala^2]A chain analogues at 12.0 × 10^{-6} and 14.0 × 10^{-6} M, respectively, in 0.001 N HCl. Included in the figure, for comparison, are the CD spectra of zinc-free bovine insulin at two concentrations, 11.40 × 10^{-6} and 1.14 × 10^{-6} M in 0.001 N HCl, pH 3.2. The analogues exhibit maxima at 193 and minima at 207, 220 (sh), and 268 (b) nm. Insulin at a comparable concentration (11.40 × 10^{-6} M) exhibits a similar CD spectrum with slightly red-shifted maxima and minima at 194.5, 208, 220–222, and 274 nm and substantially larger molar ellipticities at 195, 220, and 274 nm. The CD spectrum of insulin at 1.14 × 10^{-6} M more closely approximates the spectra of the analogues: the molar ellipticities are reduced to values not substantially larger than those observed for the analogues, and small blue shifts of the maxima and minima are observed [195 → 194 nm, 208 → 207.5 nm, 222 → 220 nm (sh), and 274 → 271 nm]. Table III records the molar ellipticities of the analogues at the aforementioned concentrations and the molar ellipticities of insulin at concentrations of (168.5–0.168) × 10^{-6} M. Insulin at 0.168 × 10^{-6} M gave quantitatively nonreproducible CD spectra, and we record (in parentheses) only the highest molar ellipticities found. We noted, however, that even at this concentration, in spite of the variability of the absolute values of molar ellipticity, the ratios remain essentially the same. We suggest that the variance in CD for very dilute insulin solutions (ca. 2 × 10^{-7} M) reflects variable loss of hormone by absorption on the glass of the cells, which could represent a significant percentage of the dissolved hormone.

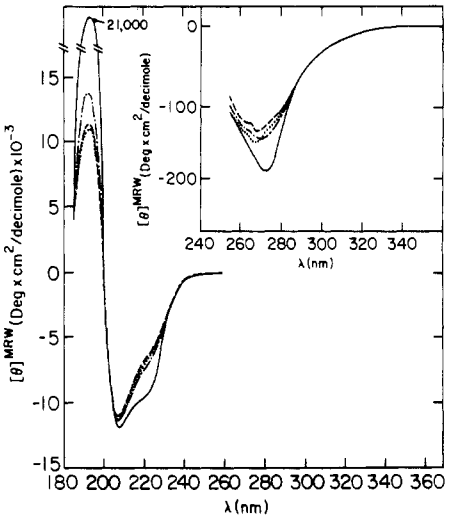

FIGURE 6: Near- and far-UV CD spectra of [Gly^2-A]insulin, (– –) 12.0 × 10^{-6} M, [Ala^2-A]insulin, (···) 14.0 × 10^{-6} M, and zinc-free insulin, (—) 11.4 × 10^{-6} M and (–·–) 1.14 × 10^{-6} M, all in 0.001 M HCl. (Inset) Zinc-free insulin, (—) 16.8 × 10^{-6} M and (–·–) 1.68 × 10^{-6} M, in 0.001 M HCl, [Gly^2-A]insulin (– –), and [Ala^2-A]insulin (···), same concentrations as shown in the main figure.

Results and Discussion

In our earlier paper (Okada et al., 1981) concerning [2-norleucine-A]insulin ([Nle^2-A]insulin), we reported the very low potency of this analogue: less than 1% compared with bovine insulin. The CD spectrum of this analogue indicated a disruption of the A^2–A^8 helical segment observed in the X-ray model of crystalline hexameric insulin (Blundell et al., 1972; Dodson et al., 1979). It was suggested that the loss of helical character of this segment would affect not only the amino acid residues within the segment but may also unfavorably modify the disposition of residues sequentially distant from this segment and involved in receptor binding. It has been postulated (Pullen et al., 1976) that residues A^1, A^5, and A^{19} are involved in receptor binding. The disruption of the A^2–A^8 helical segment of the [Nle^2]A chain analogue, we suggested (Okada et al., 1981), could be a consequence of either of two interrelated factors: (a) if norleucine was a helix breaker and/or (b) if the replacement of norleucine for isoleucine of the natural hormone interferes with the known van der Waals contact of [Ile^2]A–[Tyr^{19}]A, which is crucial for the maintenance of the helical character of this segment (Blundell et al., 1972). In either case, the disruption of the helix would affect the disposition of the A^1, A^5, and A^{19} residues. To explore these alternatives, the analogues [Gly^2-A]- and [Ala^2-A]insulins were synthesized, and their biological potency relative to that of insulin was investigated. These substitutions were chosen since the glycine residue is a known helix breaker and alanine is a helix favorer [Levitt (1981) and references cited therein]. Further, neither of these substitutions would impose additional unfavorable steric restrictions on the molecule. [Gly^2-A]insulin and [Ala^2-A]insulin assay as extremely weak full agonists, reaching the same maximum activity as insulin, but at vastly greater concentrations. [Gly^2-A]insulin displays 0.05% of the potency of the natural hormone in lipogenesis and unmeasurably low binding to the insulin receptor. [Ala^2-A]insulin is slightly more potent, assaying at 0.4% of the potency of insulin. These data show that the presence of glycine in position A^2 did indeed result in the least potent full agonist we have observed. However, the substitution of alanine in this position produced activity, although higher than that of the glycine analogue, still less than the activity of [Nle^2-A]insulin.

The reported association constants of insulin (monomer $\leftrightarrow$ dimer) are 4.0×10^4, pH 2.0 (Lord et al., 1973), and $(2.2–7.5) \times 10^5$, pH 7–8 (Goldman & Carpenter, 1974; Pocker & Biswas, 1981). Insulin then, at 1.4×10^{-6} and 16.9×10^{-6} M in 0.001 N HCl, pH 3.2, exists predominantly as the monomer and in large measure as dimer, respectively. The changes observed in the CD spectrum of insulin on dilution (Table III, Figure 6) reflect the dissociation of insulin dimer to monomer. The decrease in the molar ellipticity of insulin at 274 nm and the increase in the ratio of molar ellipticities $[\theta]_{208}/[\theta]_{222}$ on dilution of insulin solutions, which we report herein at 0.001 N HCl, have been reported at pH 7–8 and correlated with the degree of dissociation of insulin dimer (Goldman & Carpenter, 1974; Pocker & Biswas, 1980; Wood et al., 1975). We observe (Table III) that the molar ellipticity at 195 nm and the ratio $[\theta]_{195}/[\theta]_{208}$ are more sensitive measures of the extent of association of insulin. The molar ellipticity at 195 nm is reduced ca. 60%, and the ratio $[\theta]_{195}/[\theta]_{208}$ is substantially reduced: 1.7 $\rightarrow$ 1.2 for dimer vs. monomer. Calculations of the percent of helix, β-sheet, and β-bend, on the basis of the CD spectrum of dimeric insulin, are in good agreement with that found by X-ray (Provencher & Glöckner, 1981; Chang et al., 1978; Blundell & Wood, 1982). It appears reasonable to presume that the conformation of the monomeric form of insulin, as it exists in the dimer, closely corresponds to that observed in crystalline hexameric insulin. The substantial reductions in molar ellipticity at 195, 208, and 222 nm (characteristically associated with α-helix) observed following dimer dissociation (Table III) suggest that the conformation of the monomeric form of insulin in solution is different from that observed for the monomer as it exists in the dimer in solution. Pocker & Biswas (1980) have observed a substantial decrease in the molar ellipticity at 208 and 222 nm, pH 7.0, on dissociation of the dimeric form of insulin. They have attributed these changes to a conformational change in the insulin dimer to monomer transition. Recently, it was shown (Ru-chang et al., 1983) that the crystalline structure of the monomeric despentapeptide B$^{26-30}$ insulin is "closely similar to the insulin structure present in 2-Zn insulin." However, it is of interest to note that the CD spectrum of this analogue (Gattner, 1975) closely resembles that found for the A^2-substituted analogues discussed below, for porcupine insulin, shown to be monomeric (Horuk et al., 1980), as well as for monomeric insulin. Calculations by Pocker & Biswas (1980) of the percent α-helical content of the monomeric form of insulin in solution clearly indicate a substantial reduction as compared to the dimer. It seems most reasonable to speculate, in the light of the apparent paradox arising from the X-ray crystallographic results and the CD spectrum of despentapeptide B$^{26-30}$ insulin, that it is in the crystal formation that this analogue assumes a conformation similar to that of insulin and that analogously, in dimerization, monomeric insulin assumes a conformation noted in the crystalline state.

The CD spectra of [Gly^2-A]- and [Ala^2-A]insulins at $(12.0–14.0) \times 10^{-6}$ M (0.001 M HCl), respectively, are virtually identical (Figure 6; Table III). [Nle^2-A]insulin at 17.4×10^{-6} M (0.01 M HCl) is monomeric, as demonstrated by ultracentrifugal studies (Okada et al., 1981), and its CD spectrum is indistinguishable from the presently investigated analogues. Insulin at 1.14×10^{-6} M (0.001 M HCl) exists predominantly as a monomer (cf. above) and exhibits a CD spectrum that is little different from that of the analogues (Figure 6). Clearly, [Gly^2-A]- and [Ala^2-A]insulins at $(12–14) \times 10^{-6}$ M (0.001 M HCl) are predominantly, if not exclusively, monomeric.

The CD spectra of the analogues and the monomeric and dimeric forms of insulin in solution indicate that the α-helical content of these analogues is comparable to that of monomeric insulin. According to the X-ray model of the natural hormone, the segments A^2–A^8 (irregular), A^{13}–A^{19}, and B^9–B^{19} are α-helical (Blundell et al., 1972; Dodson et al., 1979). Considering that with the analogues the site of the single substitution is at A^2, it is reasonable to presume that in the analogues the A^2–A^8 helical segment is distorted. Since replacement of the A^2 isoleucine of insulin by a helix breaker, glycine, or a helix favorer, alanine, gave analogues with indistinguishable CD spectra, it may be surmised that other factors are involved in the formation and/or stabilization of the A^2–A^8 segment as an α-helix. The substantially lower molar ellipticities, at 195, 208, and 222 nm, of the monomeric form of insulin, as compared to insulin dimer, suggest, as in the case of the analogues, that the A^2–A^8 segment of monomeric insulin is also distorted. It is reasonable to suppose that it is in the formation of dimeric insulin that the A^2–A^8 segment undergoes a conformational change to an α-helical structure. The inability of the analogues to form dimers suggests that a helical A^2–A^8 segment is a stringent require-

ment for dimer formation. We suggest that dimer formation and the transition of the A^2–A^8 segment to an α-helix are interdependent and not dissociable events. The X-ray model of the natural hormone indicates a van der Waals contact between [Ile^2]A and [Tyr^{19}]A side chains (Blundell et al., 1972). We suggest that this interaction, dependent on the α-helical conformation of the A^2–A^8 segment, fixes the A^{19} tyrosine residue for favorable interaction, as seen by X-ray, with the B^{25} phenylalanine residue (Pocker & Biswas, 1981; Blundell et al., 1972). The B^{25} residue is part of the β-strands (B^{22}–B^{29}), which interact in the formation of the β-sheet characteristic of the insulin dimer. It is within the framework and coordination of these aforementioned events that we suggest that the encounter of two insulin monomers leads to the formation of a stable dimeric structure of insulin. In the case of the analogues, the interaction of the A^2 glycine, alanine, and norleucine with the A^{19} tyrosine is either aborted or not of the proper character for ensuring maintenance of the A^2–A^8 helix and the potential for dimer formation.

It is apparent that the side chain of isoleucine in position A^2 is critical for high biological activity. Isoleucine in position A^2 and tyrosine in A^{19} are among the most strongly conserved residues in various insulins (Blundell et al., 1983). The replacement of tyrosine-A^{19} with leucine gave an analogue with biological activity comparable to [Gly^2-A]insulin, little (if any) propensity for dimerization, and distortion of the helical character of the A^2–A^8 segment (unpublished results). The conformation that the insulin monomer assumes on binding to the receptor is not known. In the light of our findings with the present analogues, it appears reasonable to suppose that binding of the insulin monomer to the receptor is, as in the case of its dimerization, also dependent on the favorable interaction of the A^2 and A^{19} residues. Whether the A^2–A^8 segment of the insulin molecule is in the same helical conformation as that in the dimer could only be determined by an examination of the isolated insulin–receptor complex. It should be pointed out that the residues involved in dimer formation are not necessarily those that are involved in receptor binding. Natural insulins that do not form dimers but possess the A^2 isoleucine and A^{19} tyrosine residues [i.e., Horuk et al. (1980) and Zimmerman & Yip (1974)], although less potent than pig, bovine, and human insulins, are substantially more active than the present analogues. The interaction between the side chain of A^2 isoleucine and the phenolic ring system of A^{19} tyrosine appears to be among the most important structural features required for high biological activity in insulin. In the present analogues, the interruption of this interaction results in a conformation that has a small probability of adaptation to the conformation required for receptor binding.

Acknowledgments

We express our appreciation to Shima Joshi for technical assistance.

Registry No. I, 88932-21-2; II, 88932-22-3; III, 88932-23-4; IV, 88932-24-5; V, 88932-25-6; VI, 88932-26-7; VII, 88932-27-8; VIII, 88932-28-9; IX, 88932-29-0; X, 88932-30-3; XI, 88932-31-4; [Gly^2]A sheep insulin, 88932-20-1; [Ala^2]A sheep insulin, 23035-80-5; sheep B chain *S*-sulfonate, 18175-60-5; *N*-(benzyloxycarbonyl)-L-valyl-γ-*tert*-butyl-L-glutamic acid methyl ester, 4902-24-3; L-valyl-γ-*tert*-butyl-L-glutamic acid methyl ester, 65895-25-2; *N*-(benzyloxycarbonyl)glycine *p*-nitrophenyl ester, 1738-86-9; hydrazine hydrate, 7803-57-8; *N*-(benzyloxycarbonyl)-L-alanine *p*-nitrophenyl ester, 1168-87-2; *N*-(*tert*-butoxycarbonyl)glycyl-L-valyl-*S*-benzyl-L-cysteinyl-L-seryl-L-leucyl-L-tyrosyl-L-glutaminyl-L-leucyl-γ-benzyl-L-glutamyl-L-asparaginyl-*O*-benzyl-L-tyrosyl-*S*-benzyl-L-cysteinyl-L-asparagine *p*-nitrobenzyl ester, 87590-66-7; *N*-(*tert*-butoxycarbonyl)-L-glutaminyl-*S*-benzyl-L-cysteinyl-*S*-benzyl-L-cysteinyl-L-alanine hydrazide, 57281-63-7.

References

Blundell, T. L., & Wood, S. (1982) *Annu. Rev. Biochem. 51*, 123–154.

Blundell, T. L., Dodson, G., Hodgkin, D., & Mercola, D. (1972) *Adv. Protein Chem. 26*, 279–402.

Blundell, T. L., Bedarkar, S., & Humbel, R. E. (1983) *Fed. Proc., Fed. Am. Soc. Exp. Biol. 42*, 2592–2597.

Brown, H., Sanger, F., & Kitai, R. (1955) *Biochem. J. 60*, 556–565.

Chang, C. T., Wu, C. S. C., & Yang, J. T. (1978) *Anal. Biochem. 91*, 13–31.

Dodson, E. J., Dodson, G. G., Hodgkin, D. C., & Reynolds, C. D. (1979) *Can. J. Biochem. 57*, 469–479.

Ferderigos, N., Cosmatos, A., Ferderigos, A., & Katsoyannis, P. G. (1979) *Int. J. Pept. Protein Res. 13*, 43–53.

Ferderigos, N., Burke, G. T., Kitagawa, K., & Katsoyannis, P. G. (1983) *J. Protein Chem. 2*, 157–180.

Gattner, H. G. (1975) *Hoppe-Seyler's Z. Physiol. Chem. 386*, 1397–1404.

Goldman, J., & Carpenter, F. H. (1974) *Biochemistry 13*, 4567–4574.

Goodman, M., & Steuben, K. C. (1959) *J. Am. Chem. Soc. 81*, 3980–3983.

Hales, C. N., & Randle, P. J. (1963) *Biochem. J. 88*, 137–146.

Horuk, R., Blundell, T. L., Lazarus, N. R., Neville, R. W. J., Stone, D., & Wollmer, A. (1980) *Nature (London) 286*, 822–824.

Horvat, A., Li, E., & Katsoyannis, P. G. (1975) *Biochim. Biophys. Acta 382*, 609–620.

Iselin, B., Rittel, W. R., Sieber, P., & Schwyzer, R. (1957) *Helv. Chim. Acta 40*, 373–387.

Katsoyannis, P. G., & Tometsko, A. (1966) *Proc. Natl. Acad. Sci. U.S.A. 55*, 1554–1561.

Katsoyannis, P. G., Tometsko, A., & Zalut, C. (1966a) *J. Am. Chem. Soc. 88*, 5622–5625.

Katsoyannis, P. G., Tometsko, A., Zalut, C., & Fukuda, K. (1966b) *J. Am. Chem. Soc. 88*, 5625–5635.

Katsoyannis, P. G., Tometsko, A., Zalut, C., Johnson, S., & Trakatellis, A. C. (1967a) *Biochemistry 6*, 2635–2642.

Katsoyannis, P. G., Trakatellis, A. C., Johnson, S., Zalut, C., & Schwartz, G. (1967b) *Biochemistry 6*, 2642–2655.

Katsoyannis, P. G., Trakatellis, A. C., Zalut, C., Johnson, S., Tometsko, A., Schwartz, G., & Ginos, J. (1967c) *Biochemistry 6*, 2656–2668.

Levitt, M. (1981) *J. Am. Chem. Soc. 103*, 4277–4285.

Lord, R. S., Gubensek, F., & Rupley, J. A. (1973) *Biochemistry 12*, 4385–4390.

Okada, Y., & Katsoyannis, P. G. (1975) *J. Am. Chem. Soc. 97*, 4366–4372.

Okada, Y., Chanley, J. D., Burke, G. T., & Katsoyannis, P. G. (1981) *Hoppe-Seyler's Z. Physiol. Chem. 362*, 629–638.

Pocker, Y., & Biswas, S. B. (1980) *Biochemistry 19*, 5043–5049.

Pocker, Y., & Biswas, S. B. (1981) *J. Am. Chem. Soc. 103*, 4354–4361.

Provencher, S. W., & Glöckner, J. (1981) *Biochemistry 20*, 33–37.

Pullen, R. A., Lindsay, D. G., Wood, S. P., Tickle, I. J., Blundell, T. L., Wollmer, A., Krail, G., Brandenburg, D. Zahn, H., Gliemann, J., & Gammeltoft, S. (1976) *Nature (London) 259*, 369–373.

Ru-chang, B., Cutfield, S. M., Dodson, E. J., Dodson, G. G., Giordano, F., Reynolds, C. D., & Tolley, S. P. (1983) *Acta*

Crystallogr., Sect. B B39, 90–98.
Sanger, F., & Tuppy, H. (1951) *Biochem. J. 49*, 481–490.
Schwartz, G., & Katsoyannis, P. G. (1976) *Biochemistry 15*, 4071–4076.
Schwartz, G., Burke, G. T., & Katsoyannis, P. G. (1981) *Int. J. Pept. Protein Res. 17*, 243–255.
Schwartz, G., Burke, G. T., Chanley, J. D., & Katsoyannis, P. G. (1983) *Biochemistry 22*, 4561–4567.
Wood, S. P., Blundell, T. L., Wolmer, A., Lazarus, N. R., & Neville, R. W. J. (1975) *Eur. J. Biochem. 55*, 531–542.
Zimmerman, A. E., & Yip, C. C. (1974) *J. Biol. Chem. 249*, 4021–4025.

Influence of Vesicle Size and Oxidase Content on Respiratory Control in Reconstituted Cytochrome Oxidase Vesicles†

Thomas D. Madden,* Michael J. Hope, and Pieter R. Cullis

ABSTRACT: Previous work has shown that the respiratory control or coupling exhibited by reconstituted cytochrome oxidase systems can be markedly sensitive to the lipid composition, the lipid to protein ratio, and the vesicle size. In this work we have attempted to ascertain which, if any, of these factors plays a definitive role in determining the observed coupling. Vesicles prepared from dioleoylphosphatidylcholine–dioleoylphosphatidylethanolamine (1:4) were fractionated by DEAE chromatography to obtain a population homogeneous with respect to their lipid to protein ratio. This subpopulation was then applied to a Sepharose 4B-CL column to separate the vesicles by size. Fractions eluted from the column were assayed for enzyme activity in the presence and absence of carbonyl cyanide (trifluoromethoxy)phenylhydrazone plus valinomycin. The coupling ratio was found to be dependent upon vesicle size; the smaller the vesicles, the higher the ratio. This suggests that lipid composition per se does not determine coupling characteristics. Reducing vesicle size for a given lipid to protein ratio has two effects. First, the radius of curvature is increased and, second, the average number of oxidase molecules per vesicle is reduced. In order to identify which of these factors was responsible for the observed tighter coupling, the oxidase was reconstituted with dioleoylphosphatidylcholine into vesicles of a defined size and the number of oxidase molecules per vesicle varied. The highest coupling ratios were observed for vesicles containing on average only one oxidase dimer. As the fraction of vesicles containing more than one protein was increased, the coupling ratio rapidly declined. Mathematical analysis of these results is consistent with the proposal that in reconstituted oxidase vesicles containing two or more oxidase dimers, oxidase complexes with an inward orientation (such that they cannot interact with external cytochrome *c*) can uncouple outwardly oriented oxidase. Further, it was observed that vesicles containing a single oxidase dimer could be resolved by DEAE chromatography into subpopulations where the protein was oriented either facing outward or facing the interior of the vesicle.

Cytochrome *c* oxidase catalyzes the reduction of molecular oxygen to water, which is the terminal reaction in the mitochondrial electron transport chain. It is one of the best characterized integral membrane proteins and has been shown to be a Y-shaped multisubunit enzyme where the two arms of the Y span the inner mitochondrial membrane and the stalk (which contains the cytochrome *c* binding site) extends from the cytoplasmic side (Deatherage et al., 1982). It can be isolated and purified following detergent solubilization and can be reconstituted into vesicles with a well-defined lipid composition. It has been demonstrated that optimal activity is obtained when the enzyme is reconstituted with phospholipids that contain long unsaturated acyl groups (Vik & Capaldi, 1977).

Cytochrome oxidase serves to generate and maintain a transmembrane proton gradient in vivo, and it is therefore vital that the enzyme be well sealed in the membrane so that such gradients are not immediately dissipated. A measure of such sealing is provided by the respiratory control or coupling, given by the ratio of the enzyme activity in the presence of uncoupling agents (a proton ionophore such as FCCP[1] and the K^+ ionophore valinomycin) to that in the absence of uncouplers. Reconstituted oxidase vesicles exhibiting good respiratory control ratios can be generated (Hunter & Capaldi, 1976; Racker, 1973); however, the coupling ratios obtained are sensitive to a variety of factors. Vik & Capaldi (1977) have observed that well-coupled systems are only obtained at high lipid to protein ratios whereas other workers have shown that coupling is dependent on the lipid composition itself (Racker, 1973). Alternatively, it has been suggested that the size of the vesicle containing the oxidase may also influence respiratory control (Madden et al., 1983).

In this work we have approached this somewhat confused situation with the aim of determining whether lipid composition, protein content, or vesicle size plays a definitive role in determining the coupling ratios exhibited by reconstituted oxidase systems. We show that neither the lipid composition nor the vesicle size plays a primary role but that the oxidase content per vesicle has a marked influence. In particular, optimum coupling is obtained in vesicles containing one oxidase dimer per vesicle, and the coupling ratios decrease dramatically as the protein content is raised. These results are analyzed in terms of a model whereby in reconstituted vesicles con-

† From the Department of Biochemistry, The University of British Columbia, Vancouver, British Columbia, Canada V6T 1W5. *Received September 6, 1983.* This research was supported by the British Columbia Health Care Research Foundation. T.D.M. is a Postdoctoral Fellow of the Canadian Medical Research Council. P.R.C. is an M.R.C. Scientist.

[1] Abbreviations: DOPC, dioleoylphosphatidylcholine; DOPE, dioleoylphosphatidylethanolamine; SDS, sodium dodecyl sulfate; FCCP, carbonyl cyanide (trifluoromethoxy)phenylhydrazone; OGP, octyl β-D-glucopyranoside.

0006-2960/84/0423-1413$01.50/0